Lifetime and population of the 2S state in muonic hydrogen and deuterium

Marc Diepold,[1] Fernando D. Amaro,[2] Aldo Antognini,[1,3] François Biraben,[4] João M. R. Cardoso,[2] Daniel S. Covita,[5] Andreas Dax,[6] Satish Dhawan,[6] Luis M. P. Fernandes,[2] Adolf Giesen,[7,8] Andrea L. Gouvea,[2] Thomas Graf,[7] Theodor W. Hänsch,[1,*] Paul Indelicato,[4] Lucile Julien,[4] Cheng-Yang Kao,[9] Paul Knowles,[10] Franz Kottmann,[3] Eric-Olivier Le Bigot,[4] Yi-Wei Liu,[9] José A. M. Lopes,[2,†] Livia Ludhova,[10] Cristina M. B. Monteiro,[2] Françoise Mulhauser,[1,10] Tobias Nebel,[1] François Nez,[4] Paul Rabinowitz,[11] Joaquim M. F. dos Santos,[2] Lukas A. Schaller,[10] Karsten Schuhmann,[3,8,12] Catherine Schwob,[4] David Taqqu,[12] João F. C. A. Veloso,[5] Jan Vogelsang,[1,‡] and Randolf Pohl[1]
(CREMA Collaboration)

[1]*Max-Planck-Institut für Quantenoptik, 85748 Garching, Germany*
[2]*Departamento de Física, Universidade de Coimbra, 3004-516 Coimbra, Portugal*
[3]*Institute for Particle Physics, ETH Zurich, 8093 Zurich, Switzerland*
[4]*Laboratoire Kastler Brossel, École Normale Supérieure, CNRS, and Université P. et M. Curie – Paris 6, Case 74, Place Jussieu, 75252 Paris, CEDEX 05, France*
[5]*I3N, Departamento de Física, Universidade de Aveiro, 3810-193 Aveiro, Portugal*
[6]*Physics Department, Yale University, New Haven, Connecticut 06520-8121, USA*
[7]*Institut für Strahlwerkzeuge, Universität Stuttgart, 70569 Stuttgart, Germany*
[8]*Dausinger & Giesen GmbH, Rotebühlstr. 87, 70178 Stuttgart, Germany*
[9]*Physics Department, National Tsing Hua University, Hsinchu 300, Taiwan*
[10]*Département de Physique, Université de Fribourg, 1700 Fribourg, Switzerland*
[11]*Department of Chemistry, Princeton University, Princeton, New Jersey 08544-1009, USA*
[12]*Paul Scherrer Institute, 5232 Villigen–PSI, Switzerland*

Radiative deexcitation (RD) of the metastable 2S state of muonic hydrogen and deuterium atoms has been observed. In muonic hydrogen, we improve the precision on lifetime and population (formation probability) values for the short-lived $\mu p(2S)$ component, and give an upper limit for RD of long-lived $\mu p(2S)$ atoms. In muonic deuterium at 1 hPa, $3.1 \pm 0.3\%$ of all stopped muons form $\mu d(2S)$ atoms. The short-lived 2S component has a population of $1.35\,^{+0.57}_{-0.33}\%$ and a lifetime of $\tau_{2S}^{\text{short}}(\mu d) = 138\,^{+32}_{-34}$ ns. We see evidence for RD of long-lived $\mu d(2S)$ with a lifetime of $\tau_{2S}^{\text{long}}(\mu d) = 1.15\,^{+0.75}_{-0.53}\,\mu$s. This is interpreted as formation and decay of excited muonic molecules.

I. INTRODUCTION

When negative muons μ^- are stopped in molecular hydrogen (H_2) or deuterium (D_2) gas, muonic hydrogen or deuterium atoms (μp, μd) are formed in highly excited states with principal quantum number $n \approx 14$ [1]. Radiative and collisional deexcitation during the cascade leads to formation of muonic hydrogen atoms in the 1S ground state or the 2S metastable state [2,3]. The time interval between μ^- capture and its arrival in the 1S or 2S state is given by the so-called cascade time τ_{casc}. In muonic hydrogen, $\tau_{\text{casc}}^{\mu p}$ was measured to be 37 ± 5 ns at 0.6 hPa H_2 gas pressure [4].

The fraction of muons that actually reach the 2S state can be calculated by the observed x-ray yields during the cascade [5–8]. The fate of these atoms depends on their kinetic energy (E_{kin}): In a collision with a gas molecule, 2S atoms with $E_{\text{kin}} > 0.3$eV can end up in the short-lived 2P state which decays immediately to the ground state via Lyman-α ($K\alpha$) x-ray emission. This 0.3 eV threshold energy in the laboratory frame corresponds to the center-of-mass μp 2S-2P Lamb shift splitting of 0.2 eV. These fast deexcited 2S atoms constitute the so-called short-lived 2S component with a population $\varepsilon_{2S}^{\text{short}} = 1.70^{+0.80}_{-0.56}\%$ of all created μp atoms, and a lifetime of $\tau_{2S}^{\text{short}} = 165^{+38}_{-29}$ ns in μp at 0.6 hPa [4].

In contrast, 2S atoms with E_{kin} below the threshold constitute the so-called long-lived 2S atoms. In vacuum, the lifetime of the $\mu p(2S)$ atoms is given by the muon lifetime of $\tau_\mu \approx 2.2\ \mu$s, since the two-photon decay rate is negligibly small. In gaseous environments, collisional processes provide additional decay channels. This was first observed in μp, where a lifetime of $\tau_{2S}^{\text{long}} \approx 1\ \mu$s and a formation probability of $\varepsilon_{2S}^{\text{long}} = 1.10 \pm 0.08\%$ [9] was measured for this long-lived component at 1 hPa [10]. Such a population was imperative for the measurement of the 2S-2P Lamb shift in muonic hydrogen with laser spectroscopy [11,12].

The dominant deexcitation mechanism of the long-lived $\mu p(2S)$ atoms is via nonradiative Coulomb de-excitation (CD) in a collision, leading to $\mu p(1S)$ atoms with a E_{kin} of 900 eV [9,10,13]. Such behavior had been predicted as a result of molecular effects [14] via resonant formation of excited muonic molecular ions $[(pp\mu)^+]^*$ and their subsequent decay. This occurrence is similar to the Vesman mechanism [15] which is responsible for muon-catalyzed fusion via the formation of molecular ions from the ground state. Recently,

[*]Also at Ludwig-Maximilians-Universität, Munich, Germany.
[†]Also at Instituto Politécnico de Coimbra, ISEC, 3030-199, Portugal.
[‡]Present address: Institut für Physik, Carl von Ossietzky Universität, 26129 Oldenburg, Germany.

the molecular origin of the observed CD has been questioned, and "direct" CD in a $\mu p + \text{H}$ collision has been proposed as the source of the observed $\mu p(1S)$ atoms with E_{kin} of 900 eV [16,17].

Theoretical studies [18,19] have predicted very different behavior for excited muonic deuterium molecular ions, $[(dd\mu)^+]^*$, for which no data existed. The dominant deexcitation channel of the excited $[(dd\mu)^+]^*$ ion should be radiative deexcitation (RD) with a branching ratio (BR) around 70%, compared to only about 2% in the excited muonic hydrogen molecular ion $[(pp\mu)^+]^*$.

Here we report on the measurement of the cascade time, population, and lifetime of both the long-lived and the short-lived $2S$ states in muonic deuterium, μd, and we provide direct evidence for RD of long-lived $\mu d(2S)$ atoms. Additionally we give more precise values of the cascade time, population, and lifetime of the short-lived $2S$ state in μp and provide an upper limit for RD of long-lived $\mu p(2S)$ atoms.

II. EXPERIMENT

The data presented here were acquired during the muonic Lamb shift experiment [11,12] in 2009. For this experiment low-energy muons (3–6 keV kinetic energy) were stopped in a 20 cm long target filled with 1 hPa molecular gas (H_2 or D_2) at 20 °C. Twenty large-area avalanche photo diodes (APDs, 14×14 mm^2 active area each) [20,21] placed above and below the target served to detect x rays between $\sim$1 and 20 keV that originated from the formed muonic atoms. The 12 APDs with the best x-ray energy resolution of $\sim$21% (FWHM) at 1.9 keV and time resolution of 25 ns were used for this analysis, in order to reduce the background as far as possible.

The measured x-ray energies arise from $K\alpha$, $K\beta$, and $K \geqslant \gamma$ lines in μp (1.90, 2.25, and $\sim$2.45 keV, respectively) and μd (2.00, 2.36, and $\sim$2.58 keV), silver fluorescence lines near 3 keV, a muonic carbon line (μC; 4.75 keV), and various muonic nitrogen (μN; 1.01, 1.67, 3.08, 6.65 keV) and muonic oxygen (μO; 1.32, 2.19, 4.02, 8.69 keV) transitions. The last two contributions originate from a small leak, creating a 0.55(5)% air admixture in the target gas, that had no influence on the actual Lamb shift measurement. A silver layer on the target cell walls emitted additional delayed x rays through fluorescence upon contact with muonic atoms.

The primary background source of the experiment derives from muon decay electrons that are detected in the APDs, or in four plastic scintillators, with a time resolution of $\sim$10 ns. The offline event selection used in the analysis requires that an eligible x ray must be followed by the detection of a "delayed" high-energy electron (*del-e*) in a time window $t_e - t_X \in [0.15,6]$ μs after the x-ray time (*x-ray* + *del-e* events). Cuts on the electron identification further minimize the electron-induced background in the x-ray spectra.

III. DATA ANALYSIS AND FIT RESULTS

Following [4], we first used time-integrated *energy* spectra to determine the shape and position of each of the various $\mu p/\mu d$, Ag, μC, μN, and μO transitions, as well as shapes

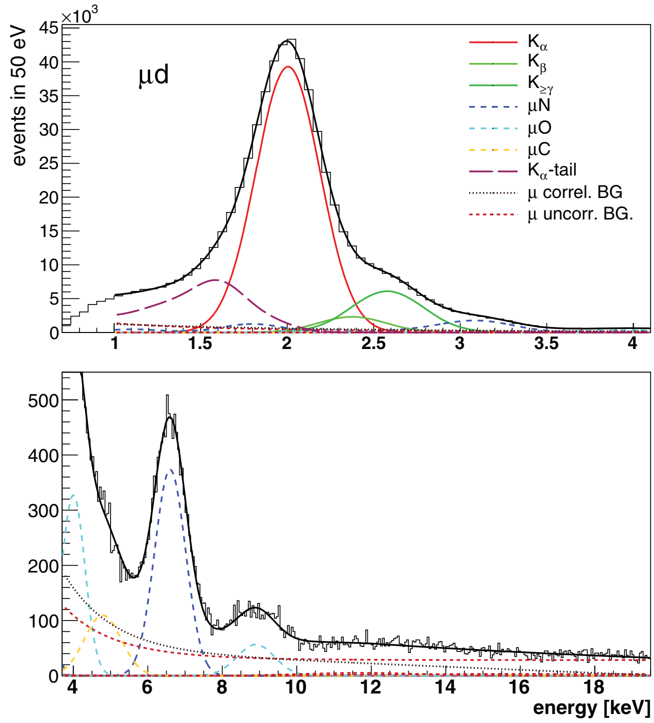

FIG. 1. (Color online) Energy spectrum of all prompt x rays in the muonic deuterium data. The plot is split to give a better overview over the contributions with low statistics.

of different background contributions. Figure 1 shows the μd data.

In a second step, we used the obtained parametrizations of the energy spectra to fit *time slices* of the *x-ray* + *del-e* energy spectrum, varying only the amplitudes of x-ray lines and backgrounds. The only exception to this is the position of the $K \geqslant \gamma$ line which was found to vary on the order of 50 eV during the time of the prompt peak, as further discussed in the Appendix.

The time-dependent x-ray amplitudes and their uncertainties gained by this procedure provide the *time spectra* of the muonic hydrogen $K\alpha$ and $K \geqslant \gamma$, μO, and μN x rays. Sixty time slices of variable length (5 ns to 1 μs, depending on the count rate) span the time up to 9 μs after muon entry. The obtained time spectra are shown in Fig. 2.

To obtain the final results, the μN, μO, and muonic hydrogen $K\alpha$ and $K \geqslant \gamma$ time spectra were fitted simultaneously (Fig. 2). The $K\beta$ spectrum was found to behave as expected but was not further considered here, because it strongly overlaps with both the $K\alpha$ and $K \geqslant \gamma$ contributions. The fit function used connects different components on the basis of prior knowledge of the muonic atom cascade:

Muon stop time: The muon stop time is given by the μN and μO time spectra, owing to the negligibly short cascade time $\sim 10^{-10}$ s for these high-Z atoms [22]. The same phenomenological shape was found to parametrize both the μN and μO time spectra with a good χ^2.

Muonic hydrogen/deuterium $K \geqslant \gamma$: The $K \geqslant \gamma$ time spectrum is obtained by convoluting the muon stop time with the $K \geqslant \gamma$ cascade time distribution. This distribution is the sum of an exponential with the time constant $\tau_{\text{casc}}^{\geqslant\gamma}$, and a sharp

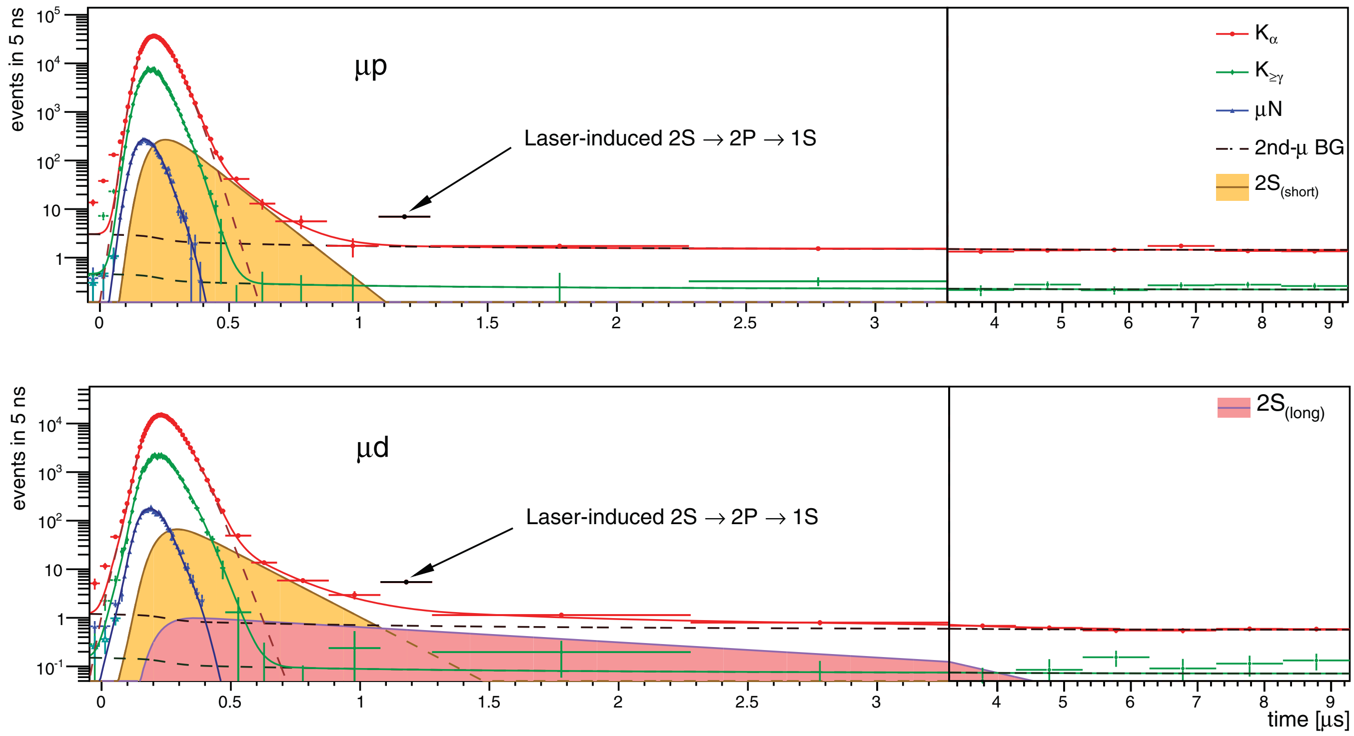

FIG. 2. (Color online) Time spectra and fits for muonic hydrogen (top) and deuterium (bottom). Note the break in the horizontal time axis. The stop time is given by the μN and μO (not shown) time spectra. The $K \geqslant \gamma$ spectrum is the stop time, convoluted with an (exponential) cascade time distribution. The $K\alpha$ spectrum in μp shows a short-lived exponential component from radiative quenching of fast $\mu p(2S)$ atoms. In μd, an additional long-lived component is visible which we consider as evidence for radiative deexcitation of long-lived $\mu d(2S)$ atoms after formation of excited molecular ions $[(dd\mu)^+]^*$. The $2S$ components are constructed by the convolution of the $K \geqslant \gamma$ distribution with exponential lifetimes (see text). In μp (μd), the prompt $K\alpha$ peak contains 881k (412k) events, and the fast component contains 11.6k (4.2k) events. The long-lived component in μd contains 440 events. The fit region starts at 0.1 μs to exclude early-time beam-correlated background.

peak at $t = 0$, as was suggested by cascade simulations [2,3]. We find $\tau_{\rm casc}^{\geqslant\gamma} = 27.7 \pm 3.0$ ns and 28.6 ± 1.9 ns for μp and μd, respectively.

Uncorrelated muons stopping in the target at random times give rise to a "2nd-μ" background in the $K \geqslant \gamma$ time spectrum which is essentially flat at times after the prompt peak. The exact shape has been deduced from the data and shows the expected decrease of event acceptance as a function of time.

Muonic hydrogen/deuterium $K\alpha$: Prompt peak and 2nd-μ background of the $K\alpha$ time spectrum are fitted similarly to the $K \geqslant \gamma$ spectrum described above, with the only exception that a purely exponential cascade time distribution is used (no peak at $t = 0$). We find a $K\alpha$ cascade time $\tau_{\rm casc}^{\alpha} = 25.0 \pm 1.5$ ns and 31.6 ± 1.7 ns in μp and μd respectively. These values agree with the respective $K \geqslant \gamma$ cascade times, so we forced them to be equal for the final analysis ($\tau_{\rm casc}^{\rm avg}$ in Table I).

In addition, $K\alpha$ x rays can originate from fast or slow RD of the metastable $2S$ state. The $2S$ state is populated from the same P states that produce the $K \geqslant \gamma$ x rays [5], and is modeled to decay (bi-)exponentially. Hence, we use a convolution of the $K \geqslant \gamma$ time spectrum with exponentials to parametrize the $2S$ signal. Short- and long-lived $2S$ atoms are modeled to give rise to a fast $[O(100\ {\rm ns})]$ and slow $[O(1\ \mu{\rm s})]$ decay time, respectively.

The time spectrum of *muonic hydrogen* is fitted very well assuming a single fast exponential from the radiatively quenched short-lived $2S$ states (Fig. 2), with a χ^2/DOF $= 252.5/247$ for the simultaneous fits of all time spectra (where DOF denotes degrees of freedom). The $K\alpha$ time spectrum alone has a χ^2/DOF of 48.8/48. The fitted amplitude $\tilde{\varepsilon}_{\rm short}(\mu p) = 1.32^{+0.42}_{-0.31}\%$ and lifetime $\tilde{\tau}_{\rm short}(\mu p) = 104^{+15}_{-13}$ ns

TABLE I. Results for μp and μd at 1 hPa. We give cascade times $\tau_{\rm casc}^{\rm avg}$, total $2S$ populations $\varepsilon_{2S}^{\rm total}$ obtained from the x-ray yields, and population $\varepsilon_{2S}^{\rm short}$ and lifetime $\tau_{2S}^{\rm short}$ of the radiatively quenched short-lived $2S$ atoms. For the population of the long-lived $\mu d(2S)$ atoms, see the text. The populations, but not the lifetimes, have been corrected for μ decay.

	μp	μd
$\tau_{\rm casc}^{\rm avg}$ (ns)	25.3 ± 1.4	31.4 ± 1.8
$\varepsilon_{2S}^{\rm total}$ (%)	2.76 ± 0.17 [7]	3.1 ± 0.3
$\varepsilon_{2S}^{\rm short}$ (%)	$1.73^{+0.56}_{-0.42}$	$1.35^{+0.57}_{-0.33}$
$\tau_{2S}^{\rm short}$ (ns)	100^{+16}_{-13}	138^{+32}_{-34}
$\varepsilon_{2S}^{\rm long}$ (%)	1.10 ± 0.08 [9]	$0.17^{+0.15}_{-0.09}$ (RD)[a]
$\tau_{2S}^{\rm long}$ (μs)	$1.04^{+0.29}_{-0.21}$ [10] (CD)	$1.15^{+0.75}_{-0.53}$ (RD)

[a]To be multiplied by $(1/0.7 \times 8)$ (see the Discussion section).

are corrected as described below to obtain the physical values in Table I.

For *muonic deuterium*, both short- and long-lived components have to be included in the $K\alpha$ fit function to achieve a $\chi^2/\mathrm{DOF} = 258.5/256$. The short-lived component has a fitted amplitude $\tilde{\varepsilon}_{\mathrm{short}}(\mu d) = 1.02^{+0.41}_{-0.23}\%$ and lifetime $\tilde{\tau}_{\mathrm{short}}(\mu d) = 142^{+29}_{-33}$ ns. The fitted amplitude of the long-lived component $\tilde{\varepsilon}_{\mathrm{long}}(\mu d) = 0.11^{+0.07}_{-0.03}\%$ is larger than zero with a significance of 3.8σ. Its fitted lifetime is $\tilde{\tau}_{\mathrm{long}}(\mu d) = 1.09^{+0.70}_{-0.49}$ μs. The physical values in Table I include all further corrections.

IV. MONTE CARLO CORRECTION

The apparatus had been optimized for the Lamb shift experiment [11,12]. For the present analysis of $2S$ lifetimes and populations, a set of corrections has to be applied to the fit results, in order to gain physical values. As the transverse target dimensions are only 16×25 mm^2, atoms in the $2S$ state may reach the target cell walls before RD occurs. Both $1S$ and $2S$ atoms may also reach the walls after x-ray emission, but before the muon decays. The high-Z target wall materials (Ag and ZnS) favor muon transfer and nuclear muon capture, reducing the μ^- decay probability and thus the *x-ray + del-e* rate. This leads to changes of the amplitudes and lifetimes of the observed x-ray signals.

A Monte Carlo (MC) simulation of the experiment was used to determine these loss correction factors of the observed signals. The simulation included the experimental E_{kin} distributions of $\mu p(1S)$ atoms [9,23], calculated cross sections for both $\mu p(1S)$ and $\mu p(2S)$ scattering and $\mu p(2S)$ quenching [17,24], as well as the evolution of the atoms' E_{kin}, the position-dependent x-ray detection efficiency, and the effect of the delayed electron time window $(t_e - t_X)$.

For muonic deuterium we adapted μp parameters with conservative systematic uncertainties. We scaled the initial E_{kin} by the reduced mass ratio, a procedure justified due to the similarity of the cascade in μp and μd [25,26]. Since elastic scattering is unimportant at the low gas pressure of 1 hPa, we also used the μp cross sections in the μd case. According to the MC simulation, detected $\mu p(2S)$ atoms experience on average only 0.7 elastic collisions before RD occurs. The $\mu p(1S)$ atoms undergo only 0.3 elastic collisions before muon decay or arrival at the target walls.

The MC simulation revealed that the fitted amplitudes $\tilde{\varepsilon}_{\mathrm{short}}$ have to be multiplied by $1.56^{+0.10}_{-0.05}$ (μp) and $1.59^{+0.20}_{-0.13}$ (μd). The fitted lifetimes of the fast components $\tilde{\tau}_{\mathrm{short}}$ are corrected by $0.96^{+0.06}_{-0.03}$ (μp) and $0.97^{+0.11}_{-0.06}$ (μd), because the fastest $2S$ atoms, which contribute most to the signal at early times, may reach the target wall before the beginning of the delayed electron time window.

V. X-RAY YIELDS

The lifetimes in Table I are physical lifetimes, corrected as detailed above, but *not* for muon decay. The physical $2S$ populations (ε) in Table I have been multiplied by $(1 - \tilde{\tau}/\tau_\mu)$, where $\tilde{\tau}$ is the fitted lifetime, to correct for muon decay ($\tau_\mu = 2.2$ μs), and by the $K\alpha$ yield $Y_{K\alpha}/Y_{\mathrm{tot}}$ to normalize to all muons. In μp, $Y_{K\alpha}/Y_{\mathrm{tot}}(\mu p) = 0.803 \pm 0.012$ at 1 hPa is interpolated from the values measured between 0.33 and 8 hPa [7].

In μd, yield measurements existed only for D_2 gas pressures $\geqslant 17$ hPa [8]. We extract the μd yields at 1 hPa from the fitted amplitudes of the prompt $K\alpha$, $K\beta$, and $K \geqslant \gamma$ peaks determined here. Using the μp data and the μp yields allows one to determine the energy-dependent APD detection efficiency. This, together with the prompt amplitudes fitted in μd, gives the μd yields at 1 hPa of $Y_{K\alpha}/Y_{\mathrm{tot}} = 0.78 \pm 0.02$, $Y_{K\beta}/Y_{\mathrm{tot}} = 0.06 \pm 0.01$, and $Y_{K\geqslant\gamma}/Y_{\mathrm{tot}} = 0.16 \pm 0.03$. As expected, the μp and μd x-ray yields are very similar [8,25,26].

VI. DISCUSSION

For muonic *hydrogen* we find a cascade time of $\tau^{\mu p}_{\mathrm{casc}} = 25.3 \pm 1.4$ ns and a radiatively quenched short-lived $2S$ population of $\varepsilon^{\mathrm{short}}_{2S}(\mu p) = 1.73^{+0.56}_{-0.42}\%$ with lifetime $\tau^{\mathrm{short}}_{2S}(\mu p) = 100^{+16}_{-13}$ ns (Table I). These values (if gas pressure difference scaling is included) agree with, yet are more precise than, those in Ref. [4].

The μp data are well fitted assuming no radiative quenching of long-lived $\mu p(2S)$ atoms. This agrees with previous observations [10] that long-lived $\mu p(2S)$ atoms quench mainly via CD, an effect explained both by direct CD [17] and molecular CD [14,18,19]. Theory predicts that an excited $[(pp\mu)^+]^*$ molecule decays mainly via CD, with a radiative BR of only 2% in muonic hydrogen [18,19], an effect too small to observe in the present experiment, or in previous searches for RD of long-lived $\mu p(2S)$ atoms [5,6].

The radiatively quenched short-lived $\mu p(2S)$ atoms observed here, $\varepsilon^{\mathrm{short}}_{2S}(\mu p) = 1.73^{+0.56}_{-0.42}\%$, and the long-lived $\mu p(2S)$ population from Ref. [9], $\varepsilon^{\mathrm{long}}_{2S}(\mu p) = 1.10 \pm 0.08\%$, sum to $\varepsilon^{\mathrm{total}}_{2S}(\mu p) = 2.8^{+0.6}_{-0.4}\%$, in agreement with the total $\mu p(2S)$ population at 1 hPa, $\varepsilon^{\mathrm{total}}_{2S}(\mu p) = 2.76 \pm 0.17\%$, calculated from the K x-ray yields [7].

For muonic *deuterium* we determine a cascade time of $\tau^{\mu d}_{\mathrm{casc}} = 31.4 \pm 1.8$ ns and a radiatively quenched short-lived $2S$ population of $\varepsilon^{\mathrm{short}}_{2S}(\mu d) = 1.35^{+0.57}_{-0.33}\%$ with lifetime $\tau^{\mathrm{short}}_{2S}(\mu d) = 138^{+32}_{-34}$ ns. The short-lived amplitude agrees with the one observed in μp.

Both the cascade time and lifetime of the short-lived $2S$ atoms scale as $\sqrt{m(\mu d)/m(\mu p)} = 1.38$, as expected for velocity-dependent collisional processes of μp and μd atoms with similar E_{kin}.

The long-lived component observed in μd is direct evidence for RD of long-lived (slow) $\mu d(2S)$ atoms. Its lifetime $\tau^{\mathrm{long}}_{2S}(\mu d) = 1.15^{+0.75}_{-0.53}$ μs is in good agreement with the CD signal lifetime observed in μp, $\tau^{\mathrm{long}}_{2S}(\mu p) = 1.04^{+0.29}_{-0.21}$ μs at 1 hPa [9,10].

The total $\mu d(2S)$ population at 1 hPa is $\varepsilon^{\mathrm{total}}_{2S}(\mu d) = 3.1 \pm 0.3\%$, calculated from the μd yields measured here. The difference $\varepsilon^{\mathrm{total}}_{2S} - \varepsilon^{\mathrm{short}}_{2S} = 1.7^{+0.4}_{-0.7}\%$ is the *expected* long-lived $\mu d(2S)$ population. It agrees with the value measured in μp, $\varepsilon^{\mathrm{long}}_{2S}(\mu p) = 1.10 \pm 0.08\%$ [9]. Also, the size of the laser-induced $2S \to 2P \to 1S$ signals (Fig. 2) proves that the long-lived 2S populations are very similar in μp

and μd. The observed long-lived amplitude, $\varepsilon_{2S}^{\text{long}} = 0.17\,^{+0.15}_{-0.09}\%$ is $\sim$10 times smaller than the expected amplitude. This can be explained via molecular formation from the excited $\mu d(2S)$ state in a collision with D_2,

$$\mu d(2S) + D_2 \rightarrow [(dd\mu)^+]^* dee. \quad (1)$$

Subsequent Auger emission of both electrons leads to the formation of a $[(dd\mu)^+]^*$ molecular ion in a ${}^1S^e$ state of the $3d\sigma_g$ potential, with vibrational quantum number $\nu = 2$ [13,18,19]. This state decays with a radiative BR of $\sim$70% into the antibinding $2p\sigma_u$ potential [18,19],

$$[(dd\mu)^+]^*_{\nu=2} \rightarrow \mu d(1S) + d + \gamma + E_{\text{kin}}. \quad (2)$$

The Franck-Condon principle predicts the x-ray spectrum in Fig. 5 of Ref. [19]. Moreover, the decay into the antibinding $2p\sigma_u$ potential produces *accelerated* $\mu d(1S)$ atoms. These can hit the walls before muon decay occurs which suppresses the observed signal amplitude for the *x-ray + del-e* event class. The MC simulation predicts that acceleration to 15 eV will give the observed factor of 1/7.

From the wave function [19,27] one finds that 27%, 8%, and 65% of the $\mu d(1S)$ atoms formed by RD from the $\nu = 2$ state acquire a E_{kin} of 2.1, 16, and 56 eV, giving signal reduction factors of 0.34, 0.10, and 0.03, respectively. This results in an overall signal reduction of 1/8, in agreement with the observed factor of 1/7.

For muonic hydrogen, the absence of a long-lived radiative component in the present data corresponds to a radiative BR that is at least 3.5 times smaller (90% C.L.) in $[(pp\mu)^+]^*$ than the one observed in $[(dd\mu)^+]^*$.

The observed lifetime of the long-lived $2S$ component, $\tau_{2S}^{\text{long}} \approx 1\ \mu$s at 1 hPa both in μp [10] and μd, is given by the excited muonic molecules formation rate [Eq. (1)] [28]. Auger emission and RD/CD [Eq. (2)] are much faster [18,19].

VII. CONCLUSION

Comparison of cascade times, yields, lifetimes, and populations of the short- and long-lived $2S$ atoms presented here shows that the cascades in muonic hydrogen and deuterium are very similar [25,26]. A notable exception is the deexcitation of the long-lived $2S$ state, which proceeds mainly via RD of $[(dd\mu)^+]^*$ molecules in μd, in contrast to CD in μp [10].

Molecular effects have proven to be important in muonic hydrogen scattering in gas targets [9,29], as well as during muon-catalyzed fusion [15,30,31]. The present analysis demonstrates the prominence of molecular effects in excited state processes of muonic hydrogen atoms. The measured formation rate of excited muonic molecules, $\lambda \approx 0.5 \times 10^6 \text{s}^{-1}$, at 1 hPa gas pressure is large, and at gas pressures approaching liquid hydrogen density, as many as 65% of the muons populate the metastable $2S$ state [3]. Hence, formation and decay of excited muonic molecules from states with $n \geqslant 2$ is expected to have a strong influence on the cascade and dynamics of muonic hydrogen isotopes [3,14].

ACKNOWLEDGMENTS

The authors thank V. P. Popov and V. N. Pomerantsev for the $\mu p(1S)$ and $\mu p(2S)$ cross sections used in the MC simulation as well as J. P. Karr and L. Hilico for the results of their calculation and fruitful discussions. We acknowledge support from the European Research Council (ERC) under Grant No. StG. 279765, the Swiss National Science Foundation (Projects No. 200020-100632 and No. 200021L-138175/1), the Swiss Academy of Engineering Sciences, the BQR de l'UFR de physique fondamentale et appliquée de l'Université Paris 6, the program PAI Germaine de Staël No. 07819NH du ministère des affaires étrangères France, and the FCT and FEDER under Grant No. SFRH/BPD/46611/2008 and Project No. FIS/82006/2006. P.I. acknowledges support by the "ExtreMe Matter Institute, Helmholtz Alliance HA216/EMMI". T.W.H. acknowledges support from the Max-Planck-Society and the Max-Planck-Foundation. Laboratoire Kastler Brossel is "UMR No. 8552" of the ENS, CNRS, and UPMC.

APPENDIX: ENERGY SHIFT OF THE $K \geqslant \gamma$ COMPONENT

While fitting the *time slices* of the *x-ray + del-e* energy spectra, it became apparent that a fixed parametrization of the $K \geqslant \gamma$ contribution was not suitable to describe the data on a satisfactory level. In order to improve the quality of the fit, the centroid energy of the $K \geqslant \gamma$ peak was treated as a free parameter in the high-statistics region of the datasets. As can be seen in Fig. 3, the energy of the $K \geqslant \gamma$ contribution is 2.49 ± 0.01 keV at times shortly after the muon entry, but then declines to 2.45 ± 0.01 keV for the latest cascade times in the case of μp. This can be explained by recollecting that muonic hydrogen atoms are created in highly exited states [1] and deexcite in the cascade through different processes [2,3]. At early times directly after muonic atom formation, $K \geqslant \gamma$ transitions start mainly from high n levels ($n \sim$ 7–12) corresponding to transition energies near the $\mu p(1S)$ dissociation energy of 2.53 keV. Lower initial n levels ($n \sim$ 4–7) dominate at later times, leading to the corresponding lower transition energies.

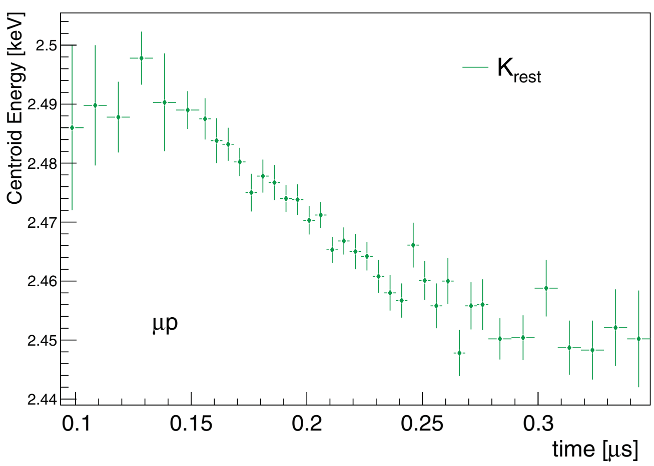

FIG. 3. (Color online) Centroid energy of the $K \geqslant \gamma$ component as obtained by the fit of the μp dataset between 0.1 and 0.4 μs after muon entry.

[1] M. Leon and H. A. Bethe, Phys. Rev. **127**, 636 (1962).
[2] T. S. Jensen and V. E. Markushin, Eur. Phys. J. D **21**, 261 (2002).
[3] T. S. Jensen and V. E. Markushin, Eur. Phys. J. D **21**, 271 (2002).
[4] L. Ludhova *et al.*, Phys. Rev. A **75**, 040501 (2007).
[5] H. Anderhub *et al.*, Phys. Lett. B **71**, 443 (1977).
[6] P. O. Egan, S. Dhawan, V. W. Hughes, D. C. Lu, F. G. Mariam, P. A. Souder, J. Vetter, G. zuPutlitz, P. A. Thompson, and A. B. Denison, Phys. Rev. A **23**, 1152 (1981).
[7] H. Anderhub *et al.*, Phys. Lett. B **143**, 65 (1984).
[8] M. Bregant *et al.*, Phys. Lett. A **241**, 344 (1998).
[9] R. Pohl, Ph.D. thesis, ETH Zurich, Switzerland, 2001, online at http://e-collection.ethbib.ethz.ch.
[10] R. Pohl *et al.*, Phys. Rev. Lett. **97**, 193402 (2006).
[11] R. Pohl *et al.*, Nature (London) **466**, 213 (2010).
[12] A. Antognini *et al.*, Science **339**, 417 (2013).
[13] R. Pohl *et al.*, Hyperfine Interact. **138**, 35 (2001).
[14] P. Froelich and A. Flores-Riveros, Phys. Rev. Lett. **70**, 1595 (1993).
[15] E. A. Vesman, Pis'ma Zh. Eksp. Teor. Fiz. **5**, 113 (1967) [JETP Lett. **5**, 91 (1967)].
[16] G. Ya. Korenman, V. N. Pomerantsev, and V. P. Popov, JETP Lett. **81**, 543 (2005).
[17] V. P. Popov and V. N. Pomerantsev, Phys. Rev. A **83**, 032516 (2011).
[18] E. Lindroth, J. Wallenius, and S. Jonsell, Phys. Rev. A **68**, 032502 (2003); **69**, 059903(E) (2004).
[19] S. Kilic, J.-P. Karr, and L. Hilico, Phys. Rev. A **70**, 042506 (2004).
[20] L. Fernandes *et al.*, Nucl. Instrum. Methods A **498**, 362 (2003).
[21] L. Ludhova *et al.*, Nucl. Instrum. Methods. A **540**, 169 (2005).
[22] L. Bracci and G. Fiorentini, Nuovo Cimento A **43**, 9 (1978).
[23] F. Kottmann *et al.*, Hyperfine Interact. **119**, 3 (1999).
[24] V. P. Popov and V. N. Pomerantsev (private communication).
[25] B. Lauss *et al.*, Phys. Rev. Lett. **80**, 3041 (1998).
[26] B. Lauss *et al.*, Phys. Rev. A **60**, 209 (1999).
[27] J.-P. Karr and L. Hilico (private communication).
[28] J. Wallenius, S. Jonsell, Y. Kino, and P. Froelich, Hyperfine Interact. **138**, 285 (2001).
[29] A. Adamczak *et al.*, At. Data Nucl. Data Tables **62**, 255 (1996).
[30] L. I. Ponomarev, Contemp. Phys. **32**, 219 (1990).
[31] D. Balin *et al.*, Phys. Part. Nucl. **42**, 185 (2011).